# Structural evidence of polymorphism and conformational isomorphism of a somewhat flexible molecule: M-anisic acid

**ARTICLE** *in* JOURNAL OF THERMAL ANALYSIS AND CALORIMETRY · APRIL 2015

Impact Factor: 2.04 · DOI: 10.1007/s10973-014-4289-y



**7 AUTHORS**, INCLUDING:

P. S. Pereira Silva
University of Coimbra
**75** PUBLICATIONS **209** CITATIONS
SEE PROFILE

Ricardo Castro
University of Coimbra
**33** PUBLICATIONS **240** CITATIONS
SEE PROFILE

João Canotilho
University of Coimbra
**26** PUBLICATIONS **156** CITATIONS
SEE PROFILE

Ermelinda eusébio
University of Coimbra
**47** PUBLICATIONS **255** CITATIONS
SEE PROFILE

J Therm Anal Calorim (2015) 120:667–677
DOI 10.1007/s10973-014-4289-y

# Structural evidence of polymorphism and conformational isomorphism of a somewhat flexible molecule: *m*-anisic acid

**Pedro S. Pereira Silva · Ricardo A. E. Castro · Elodie Melro · Manuela Ramos Silva · Teresa M. R. Maria · João Canotilho · M. Ermelinda S. Eusébio**

Received: 29 May 2014 / Accepted: 4 November 2014 / Published online: 27 December 2014


**Abstract** *m*-Anisic acid is generally recognized as a safe (GRAS) flavouring substance. Its GRAS status and the functional groups present in the molecule make it an interesting candidate for pharmaceutical co-crystallization studies. The knowledge of *m*-anisic acid crystalline structure/polymorphic behaviour is important information for its applications. In this work, a crystalline structure of *m*-anisic acid form I, $T_{fus} = 105$ °C, was solved by X-ray diffraction: monoclinic, space group $P2_1/n$, with $a = 13.8075(5)$ Å, $b = 5.0221(2)$ Å, $c = 21.4455(8)$ Å, $\beta = 99.325(3)°$, $Mr = 331.37$, $V = 1467.44(10)$ Å$^3$, $Z = 8$ and $R = 0.0395$ (CCDC No. 985352). A recent paper by Raffo et al. (J Mol Struct 1070:86–93, 2014) (CCDC No. 985637) also resolved the structure, and within experimental error, the two structures are equal. The molecular flexibility of *m*-anisic acid results in the presence of two conformers in the unit cell, a rare case of conformational isomorphism. These two conformers were found by ab initio calculations to differ in energy by 4.9 kJ mol$^{-1}$. Solid samples were generated by crystallization from solutions and by melt cooling. Using a multidisciplinary approach involving thermal analysis (DSC, PLTM), infrared spectroscopy and X-ray powder diffraction, a new monotropic solid form II, $T_{fus} = 94$ °C, was identified and characterized. Polymorph II slowly transforms into polymorph I at room temperature.

**Keywords** 3-Methoxybenzoic acid · *m*-Anisic acid · Polymorphism · GRAS · Thermal analysis · Ab initio calculations · Fingerprint plots

P. S. Pereira Silva (✉) · M. R. Silva
CEMDRX, Physics Department, University of Coimbra, 3004-516 Coimbra, Portugal
e-mail: psidonio@pollux.fis.uc.pt

R. A. E. Castro (✉) · J. Canotilho
CEF, Faculty of Pharmacy, University of Coimbra, 3000-548 Coimbra, Portugal
e-mail: rcastro@ff.uc.pt

E. Melro · T. M. R. Maria · M. E. S. Eusébio
CCC, Department of Chemistry, University of Coimbra, 3004-535 Coimbra, Portugal

## Introduction

Our interest in the solid-state chemistry of methoxybenzoic acids, also known as anisic acids, Fig. 1, comes from an ongoing project dealing with pharmaceutical co-crystals. The best co-formers for the synthesis of these new solid forms, which are of interest in the pharmaceutical and food industries, must be selected. Anisic acids are excellent candidates. These compounds occur naturally in *Pimpinella anisum* and are used as flavouring agents, according to the European Food Safety Authority [1] and the World Health Organization [2]. The most widely employed isomer is *p*-anisic acid, which is also used as a preservative of fragrance in cosmetic formulations [3–6]. Some thermodynamic data are available for the three isomers [7], and *p*-anisic acid is recommended as an organic reference material for temperature calibration in differential scanning calorimetry [8]. Crystalline structures of *o*-anisic acid [9] and of *p*-anisic acid [10] are already available in literature. Very recent data, however, with a CCDC number superior to ours, could be found for *m*-anisic acid [11] but without any reference to polymorphism.

It is known that approximately one-third of organic compounds exhibit polymorphism [12], "Polymorphism is a solid crystalline phase of a given compound resulting from the possibility of at least two crystalline arrangements of the molecules of that compound in the solid state" [13].

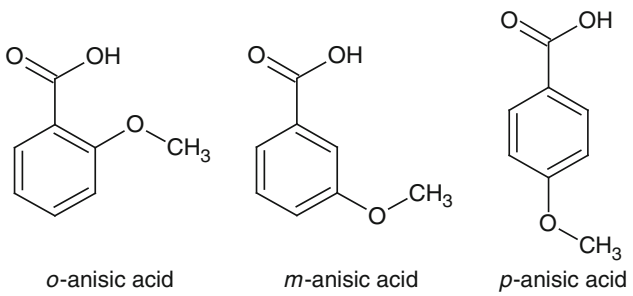


**Fig. 1** Anisic acid isomers

Conformationally flexible molecules have more degrees of freedom than rigid molecules, such that a greater scope for polymorphism might be expected with them. *m*-Anisic acid is a small molecule that has some degree of conformational flexibility. This property sometimes leads to *conformational polymorphism*, the occurrence of different conformers in distinct polymorphic structural modifications or more rarely to *conformational isomorphism*, the occurrence of different conformers in the same crystal structure [14–16].

Being a GRAS flavouring substance [17], *m*-anisic acid aroused our attention as an interesting potential co-former in co-crystallization studies. Based on the absence in the literature of resolved crystal structures, thermal behaviour studies, spectroscopic data or computational studies on this system, research on the polymorphism of *m*-anisic acid is likely to be relevant both when it is used alone and also for a correct co-crystal synthesis interpretation. In this paper, an investigation of *m*-anisic acid polymorphism is undertaken using thermal analysis (DSC and PLTM), infrared spectroscopy, X-ray diffraction and DFT calculations.

## Materials and methods

### Materials

3-Methoxybenzoic acid was acquired from Sigma-Aldrich (*m*-anisic acid, 99 %, lot 13920MC-435A). The commercialized compound was slightly brownish and was purified by sublimation at 75 °C under reduced pressure ($P = 103$ Pa). The resulting compound was white and crystalline. Samples were also prepared by crystallization from solutions and by grinding. In crystallization experiments, typically 10–20 mg of *m*-anisic acid was used in 2 mL of analytical grade solvents. After filtration onto a Petri dish, the solvent was evaporated, either at room temperature or at 2 °C. A Retsch MM400 mill with a 10 mL stainless steel grinding jar and two 7 mm diameter stainless steel balls per jar was used for grinding. A total mass of about 50 mg was ground for 30 min at a frequency of 15 Hz.

### Polarized light thermal microscopy (PLTM)

The solids were characterized by PLTM using a Linkam hot stage system, model DSC600, with a Leica DMRB microscope and a Sony CCD-IRIS/RGB video camera. A Real-Time Video Measurement System software from Linkam was used for image analysis. The images were obtained by combined use of polarized light and wave compensators, using 200× magnification.

### Differential scanning calorimetry (DSC)

The studies were performed on a PerkinElmer Pyris1 power compensation calorimeter with an intracooler cooling unit at −25 °C [ethylene glycol/water, 1:1 (v/v), cooling mixture]. The samples, mass ~1.5 mg, were hermetically sealed in 30 μL aluminium pans, and an empty pan was used as reference. A 20-mL $min^{-1}$ nitrogen purge was employed. Temperature calibration [18, 19] was performed with the high-grade standards biphenyl (CRM LGC 2610, $T_{fus} = 68.93(3)$ °C, benzoic acid (CRM LGC 2606, $T_{fus} = 122.35(2)$ °C), indium (Perkin-Elmer, $x = 99.99$ %, $T_{fus} = 156.60$ °C) and caffeine (Mettler Toledo calibration substance, ME 18 872, $T_{fus} = 235.6(2)$ °C). Enthalpy calibration was performed with indium $\Delta_{fus}H = 3286(13)$ J $mol^{-1}$ [18].

### Infrared spectroscopy (FTIR)

Spectra of the solids were recorded at room temperature with the KBr pellet technique using a ThermoNicolet IR300 FTIR spectrometer, resolution 1 $cm^{-1}$, 32 scans and a PerkinElmer Spectrum 400 FTIR/ATR diamond/zinc selenide plate, resolution 1 $cm^{-1}$, 32 scans.

### Single-crystal X-ray diffraction (SXD)

A crystal of the title compound obtained by crystallization in water solution at room temperature, with a plate habit and having approximate dimensions of 0.38 mm × 0.18 mm × 0.08 mm, was glued on a glass fibre and mounted on a Bruker Apex II diffractometer. Diffraction data were collected at room temperature 293(2) K using graphite monochromated Mo $K\alpha$ radiation ($\lambda = 0.71073$ Å). Data reduction was performed with APEX II [20]. Lorentz and polarization corrections were applied. Absorption correction was applied using SADABS [21].

The crystal structure was solved with direct methods using SHELXS-97 programme [22] and refined on $F^2$ by full-matrix least squares with SHELXL-97 programme [22]. The anisotropic displacement parameters for non-hydrogen atoms were applied. Carboxylic hydrogen atoms were located in a difference Fourier map, and their coordinates were refined with $U_{iso}(H) = 1.5U_{eq}(O)$ and

the O–H bond lengths restrained to 0.82 Å. The other hydrogen atoms were placed at calculated positions and refined with isotropic parameters as riding atoms using SHELXL-97 defaults. The final least-squares cycle was based on 3521 observed reflections [$I > 2\ \sigma(I)$], 207 variable parameters, converged with $R = 0.0395$ and $wR = 0.1049$. Supplementary data have been deposited at the Cambridge Crystallographic Data Centre (CCDC No. 985352).

### X-ray powder diffraction (XRPD)

The single crystals were powdered thoroughly using a pestle and mortar to prepare a polycrystalline sample. The sample powder was sifted with a 63 $\mu$m sieve, and glass capillaries (0.5 mm diameter) were filled with the powdered specimens. The samples were mounted on an ENRAF-NONIUS powder diffractometer (equipped with a CPS120 detector from INEL), and data were collected for 15 min to 1 h using Debye–Scherrer geometry. Monochromatized Cu $K_{\alpha 1}$ radiation was used ($\lambda = 1.5406$ Å). Silicon was chosen as an external calibrant. Samples were heated/cooled by a hot/cold nitrogen gas stream (Oxford Cryosystems, series 600) at 6 °C min$^{-1}$. One data collection of 48 h at room temperature was also performed for the Rietveld refinement.

### Ab initio calculations

The geometry optimizations were performed using the Firefly QC package [23], which is partially based on the GAMESS (US) source code [24], starting from the experimental X-ray geometries of molecules A and B. The calculations were performed within density functional theory (DFT) using Becke three-parameter Lee–Yang–Parr (B3LYP) for exchange and correlation, which combines the hybrid exchange functional of Becke [25, 26] with the correlation functional of Lee, Yang and Parr [27]. The calculations were performed with the Pople's 'triple split' 6-311G(d,p) basis set, which includes a set of *p*-polarization functions for the H atoms and a set of *d*-polarization functions for the C and O atoms. Each self-consistent field calculation was iterated until a $\Delta\rho$ of less than $10^{-5}$ bohr$^{-3}$ was achieved. The final equilibrium geometries at the minimum energy had a maximum gradient in internal coordinates of $10^{-5}$ hartree bohr$^{-1}$ or hartree rad$^{-1}$. At the end of these geometry optimizations, Hessian calculations were carried out to guarantee that the final structures correspond to true minima using the same level of theory as in the geometry optimizations. DFT calculations have also been performed of the single point energy for the experimental X-ray geometries of the two independent molecules A and B, using the method described above (B3LYP functional, 6-311G(d,p) basis set), to determine the energy difference between the two geometries in the crystal.

## Results and discussion

### Crystal structure of polymorph I

Good quality single crystals allowed the determination of a crystalline structure by single-crystal X-ray diffraction, hereafter identified as polymorph I (Table 1). During the preparation of our manuscript, another group determined almost simultaneously (CCDC No. 985637) the crystal structure of polymorph I [11]. Within experimental error, the two structures are equal.

Polymorph I crystallizes in the space group $P2_1/n$, with two molecules (A and B) in the asymmetric unit (Fig. 2). In 2000, Steiner [28] indicated the existence of systems with $Z' > 1$ as a relatively rare occurrence for organic molecules (10.8 % of CSD structures out of 2000). A recent

**Table 1** Crystal data and structure refinement parameters for *m*-anisic acid polymorph I

| | |
|---|---|
| Empirical formula | $C_8H_8O_3$ |
| fw | 152.14 |
| Temperature/K | 293(2) |
| Wavelength/Å | 0.71073 |
| Cryst syst | Monoclinic |
| Space group | $P2_1/n$ |
| *a*/Å | 13.8075(5) |
| *b*/Å | 5.0221(2) |
| *c*/Å | 21.4455(8) |
| $\beta$/° | 99.325(3) |
| Volume/Å$^3$ | 1467.44(10) |
| *Z* | 8 |
| Calc density/g cm$^{-3}$ | 1.377 |
| Abs coeff/mm$^{-1}$ | 0.106 |
| $F_{000}$ | 640 |
| Crystal habit, colour | Plate, colourless |
| Crystal size/mm | 0.38 × 0.18 × 0.08 |
| $\theta$ range for data collection/° | 2.99–27.94 |
| Index ranges | $-17 < h < 18$, $-6 < k < 6$, $-26 < l < 28$ |
| Reflns collected/unique | 46897/3521 |
| Completeness to $\theta_{max}$/% | 99.9 |
| Refinement method | Full-matrix least squares on $F^2$ |
| Data/restraints/parameters | 3521/2/207 |
| Goodness-of-fit on $F^2$ | 1.024 |
| Final *R* indices [$I > 2\sigma(I)$] | $R_1 = 0.0395$, $wR_2 = 0.1049$ |
| *R* indices (all data) | $R_1 = 0.0600$, $wR_2 = 0.1190$ |
| Largest diff peak and hole/e Å$^{-3}$ | 0.204 and −0.202 |

inspection to the CCDC database [CSD version 5.34 updates (Nov 2012)] shows the existence of 56950 compounds (organic and organometallic), with $Z' > 1$, out of 630919 compounds (9.0 %). The origin of this phenomenon (the presence of multiple molecules in the asymmetric unit) is still a matter of much discussion within the scientific community [29, 30]. The molecules are essentially planar, with the carboxyl and the methoxy groups almost in the plane of the benzene ring. The maximum deviations from the least-squares planes of molecules A and B are 0.029(1) Å for the O1A atom and 0.040(1) Å for the C8B atom. Selected structural parameters can be seen in Table 2.

The bond lengths in the carboxyl group are similar, suggesting some charge delocalization between the two C7–O bonds. This may indicate a small degree of rotational disorder in the carboxyl group, a situation that is common in carboxylic acids. However, the residual charges located near the O1 atoms are small (about 0.16 e $Å^{-3}$), and for this reason, it was not considered necessary to refine a disorder model.

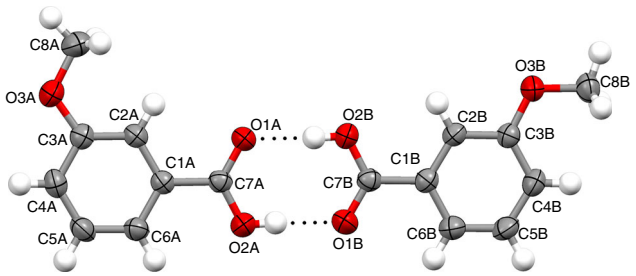


**Fig. 2** Hydrogen-bonded dimer of symmetry-independent molecules A and B of *m*-anisic acid polymorph I. *Ellipsoids* are drawn at the 50 % probability level

**Table 2** Comparison of selected geometrical parameters for *m*-anisic acid polymorph I as determined by X-ray diffraction and from DFT geometry optimizations for the symmetry-independent molecules A and B

| | Experimental | | DFT | |
|---|---|---|---|---|
| | Molecule A | Molecule B | Molecule A | Molecule B |
| Bond lengths/Å | | | | |
| O1–C7 | 1.2556(14) | 1.2475(15) | 1.2086 | 1.2066 |
| O2–C7 | 1.2740(15) | 1.2827(15) | 1.3562 | 1.3570 |
| O3–C3 | 1.3641(16) | 1.3605(15) | 1.3611 | 1.3621 |
| O3–C8 | 1.4183(18) | 1.4286(16) | 1.4227 | 1.4208 |
| C1–C7 | 1.4844(17) | 1.4858(17) | 1.4875 | 1.4893 |
| Bond angles/° | | | | |
| O1–C7–O2 | 123.40(11) | 122.97(12) | 121.88 | 122.03 |
| C3–O3–C8 | 118.10(11) | 117.62(10) | 118.30 | 118.56 |
| Dihedral angles/° | | | | |
| O2–C7–C1–C6 | 1.69(18) | 179.98(12) | −0.10 | 179.95 |
| C2–C3–O3–C8 | −1.4(2) | −176.75(11) | −0.06 | 179.97 |

The orientation of the methoxy group is quite different in the two symmetry-independent molecules. Considering Newman projections along the C3–O3 bonds, in molecule A atom C8 eclipses ring atom C2 ($\phi_{C2–C3–O3–C8} = -1.4(2)°$), whereas in molecule B, it eclipses the ring atom C4 ($\phi_{C2–C3–O3–C8} = -176.75(11)°$).

The symmetry-independent molecules A and B are hydrogen bonded in pairs through the carboxyl groups (see Fig. 3; Table 3), forming rings of descriptor $R_2^2(8)$ according to Etter's graph-set theory [31, 32]. The molecules in these dimers are almost coplanar. The crystal structure is build up from dimers in two different orientations which are approximately perpendicular to each other, with the angle between the least-squares planes being 83.8° (see Fig. 4). The crystal packing is also stabilized by a weak C–H···$\pi$ interaction where the C4A–H4A bond points towards the edge of the aromatic ring of molecule B, with a H···$\pi^i$ distance of 3.60 Å and a C–H···$\pi$ angle of 149° [symmetry code: (i) $x - 1, y, z$].

### *Fingerprint plots*

Hirshfeld surfaces and fingerprint plots [33, 34] are powerful tools for visualizing and exploring intermolecular interactions. This is important when the same molecule is in different crystalline environments, as in the case of polymorphism of molecular materials or of crystal structures with more than one molecule in the asymmetric unit ($Z' > 1$).

The intermolecular interactions of the two independent molecules were analysed by the two-dimensional fingerprint plots [34] derived from Hirshfeld surfaces [33], using CrystalExplorer version 3.1 [35]. 2D-fingerprint plots were generated from the $d_i$ and $d_e$ pairs measured on each individual spot of the calculated Hirshfeld surface. The two-dimensional fingerprint plots for the independent molecules A and B are presented in Fig. 5. The fingerprint plots have the same basic features, with both showing the presence of a pair of long sharp spikes, a characteristic of strong hydrogen bonds, in this case the O–H···O hydrogen bonds. The two polymorphs feature a diffuse region of blue points between the hydrogen bond spikes, which is characteristic of the cyclic hydrogen bond dimer motif.

The main difference between the two fingerprint plots is the relative spread of data points at high $d_i$ and $d_e$ in molecule B, which is related to the different orientation of the methoxy group, which points away from the ring in this structure.

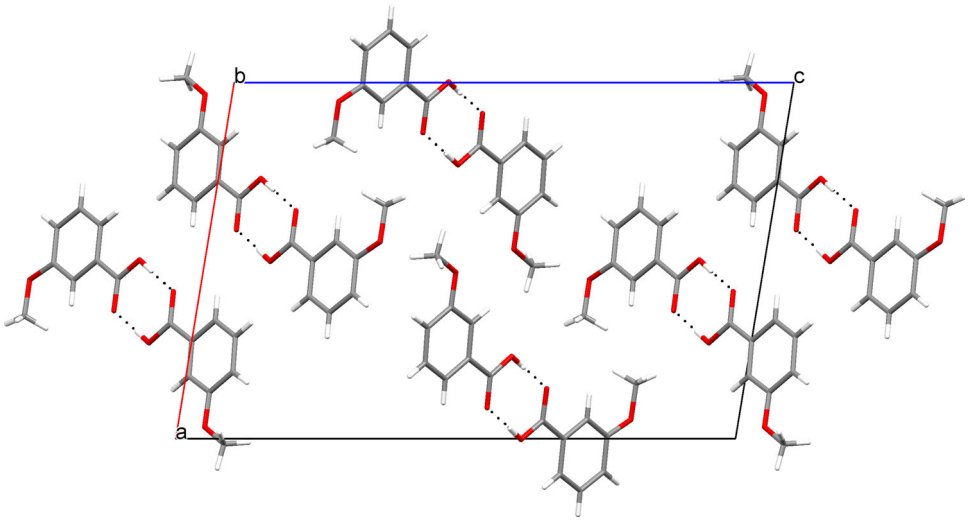


**Fig. 3** Packing diagram of *m*-anisic acid polymorph I viewed along the *b*-axis. H bonds are drawn as *dashed lines*

**Table 3** Hydrogen bonds parameters of *m*-anisic acid polymorph I

| | D–H/Å | H···A/Å | D···A/Å | D–H···A/° |
|---|---|---|---|---|
| O2A–H2A1···O1B$^{i}$ | 0.833(9) | 1.793(10) | 2.6229(14) | 174(2) |
| O2B–H2B1···O1A$^{ii}$ | 0.845(9) | 1.809(10) | 2.6515(13) | 175(2) |

Symmetry codes i: $x + 1/2, -y + 5/2, z + 1/2$; ii: $x - 1/2, -y + 5/2, z - 1/2$

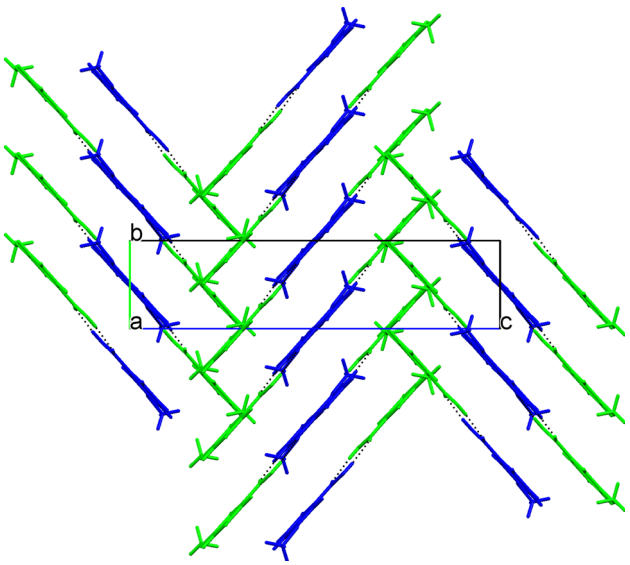


**Fig. 4** A view down the *a* axis of the unit cell of *m*-anisic acid polymorph I with the molecules coloured by symmetry equivalence: *green* molecule A, *blue* molecule B. (Color figure online)

### *Ab initio calculations*

To get some insight on the influence of the intermolecular interactions on the molecular geometries, DFT calculations of the equilibrium geometries were performed for molecules A and B in vacuum. These DFT calculations closely reproduce the solid-state geometry of the two molecules (Table 2). The agreement between the experimental and calculated bond lengths and valence angles is very good, except for the C7–O bond lengths where the differences may be explained by the charge delocalization due to a small degree of rotational disorder in the carboxyl group, as mentioned above.

The energy difference between molecules A and B is just 4.90 kJ mol$^{-1}$, with the B conformation being the more stable. This energy difference is comparable to the energies involved in rotations about single bonds [36]. Intermolecular interactions can easily account for this relative low conformational energy difference since hydrogen bond strengths are generally estimated to be in the range of 2–63 kJ mol$^{-1}$ [37]. The molecular geometric parameters most likely to be affected by these interactions are the torsion angles around single bonds, as is the case of these two conformers.

## Evidence of a new polymorphic form

### *Thermal behaviour*

Polymorph I, acquired commercially and purified by sublimation, was studied in heating/cooling cycles by DSC, Fig. 6 and Table 4. In the first heating run, polymorph I melts at 105.4 °C, and no other events are observed. A supercooling value of about 25 °C, typical for organic compounds [38], is registered on cooling at a scanning rate of 10 °C min$^{-1}$. The resulting solid submitted to another heating run melts at 94.0 °C—melt crystallization gives rise to a new solid form, polymorph II.

After melt crystallization in a DSC pan, a second heating run performed 15 days after shows a small peak of form I, and 6 months later shows that about 10 % of polymorph II was transformed into polymorph I, while

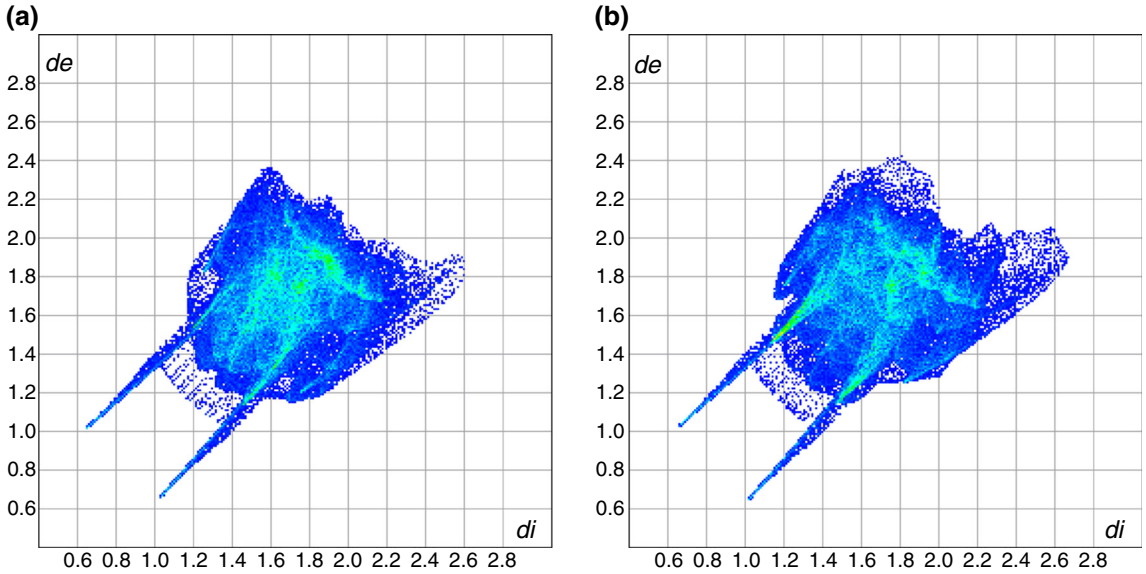


**Fig. 5** 2D fingerprint plots for the independent molecules A and B in the crystalline structure of *m*-anisic acid polymorph I

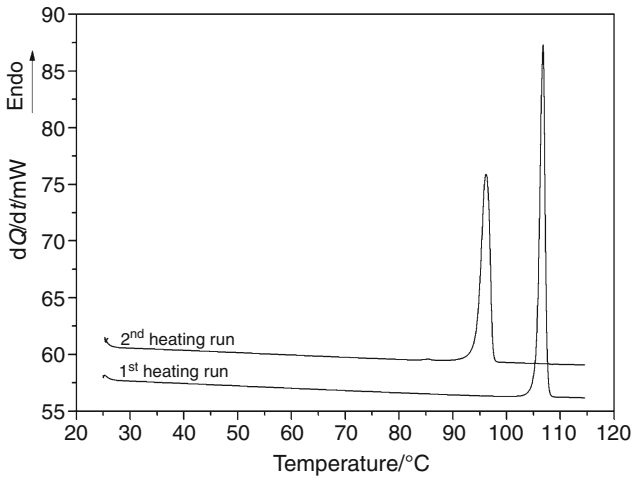


**Fig. 6** Illustrative DSC curves of the first and second heating runs of *m*-anisic acid ($m = 1.51$ mg, $\beta = 10$ °C min$^{-1}$)

2 years later a complete transformation was observed, Fig. 7.

The effect of milling on the solid samples is an essential step in the green synthesis of co-crystals as it may induce polymorphic transitions. The knowledge of the occurrence of these transitions in the pure components is very important for the correct interpretation of co-crystal synthesis data. For *m*-anisic acid, the milling process (mechanical milling or even using a pestle and mortar) induces the polymorphic transition of polymorph II into polymorph I.

*X-ray powder diffraction*

A Rietveld refinement [39] was performed with Fullprof software [40] using a powder diffractogram collected at

**Table 4** Thermodynamic parameters from DSC curves obtained on heating and cooling runs of *m*-anisic acid

| | $T_{onset}$/°C | $\Delta_{trs}H$/kJ mol$^{-1}$ | |
|---|---|---|---|
| 1st Heating | 105.4(2) | 23.2(6) | $n = 5$ |
| 1st Cooling | 81.1(8) | −19.0(1) | $n = 5$ |
| 2nd Heating | 94.0(4) | 19.8(6) | $n = 4$ |

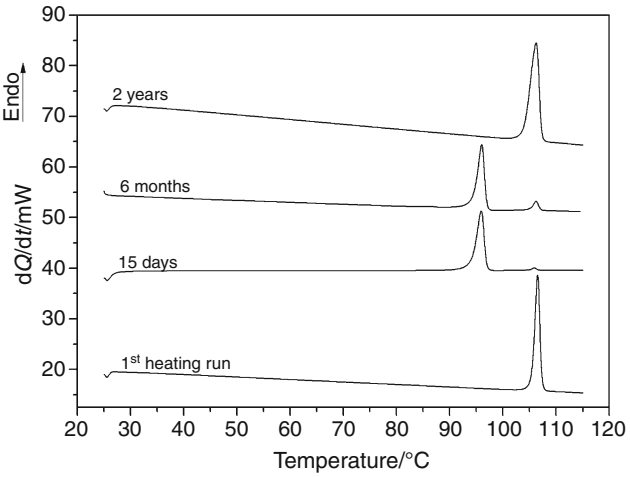


**Fig. 7** DSC heating curves showing the ageing effect on polymorph II of *m*-anisic acid

room temperature over a 48-h period. The overall parameters, such as cell parameters, $2\theta$ zero, scale factor, full-width at half-maximum and asymmetry parameter, were allowed to refine in the range of 5°–45°, with a final Bragg reliability factor of 13.5 %. The agreement between experimental and calculated patterns (see Fig. 8) confirms

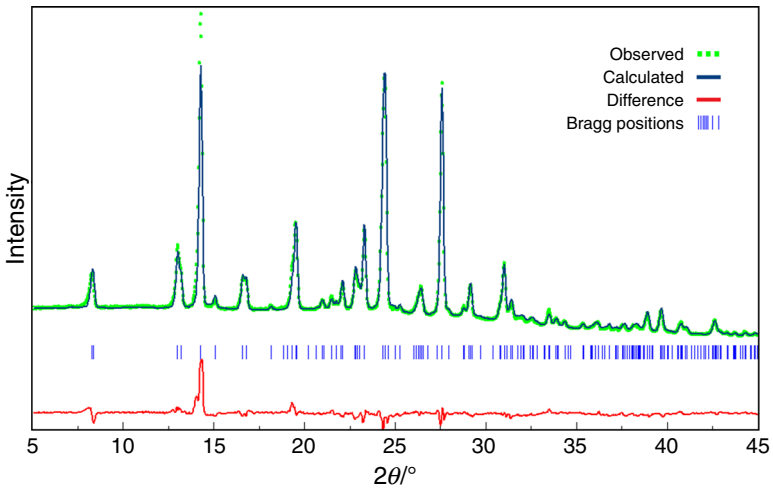


**Fig. 8** Results from a least-squares fit using the Rietveld method: experimental powder diffraction pattern (*green*); simulated diffraction pattern of polymorph I using the Rietveld method (*dark-blue*); difference between the observed and calculated intensities (*red*) and corresponding Bragg positions (*blue*). (Color figure online)

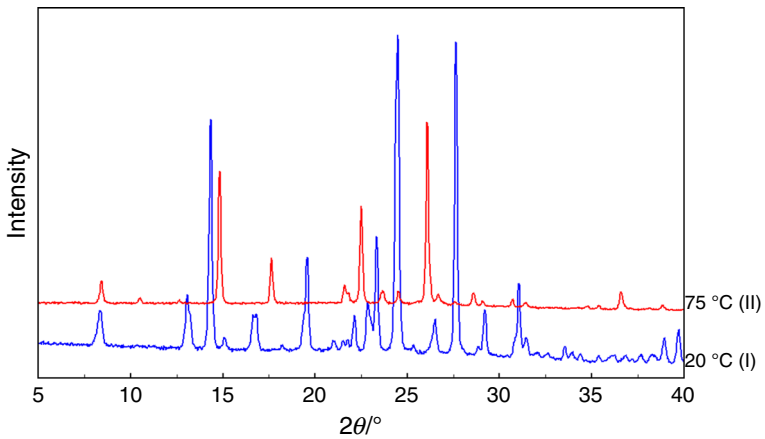


**Fig. 9** Powder X-ray diffractograms of *m*-anisic acid polymorph I (*blue* crystallized in water at room temperature collected at 20 °C) and II (*red* cooled from the melt to 75 °C). (Color figure online)

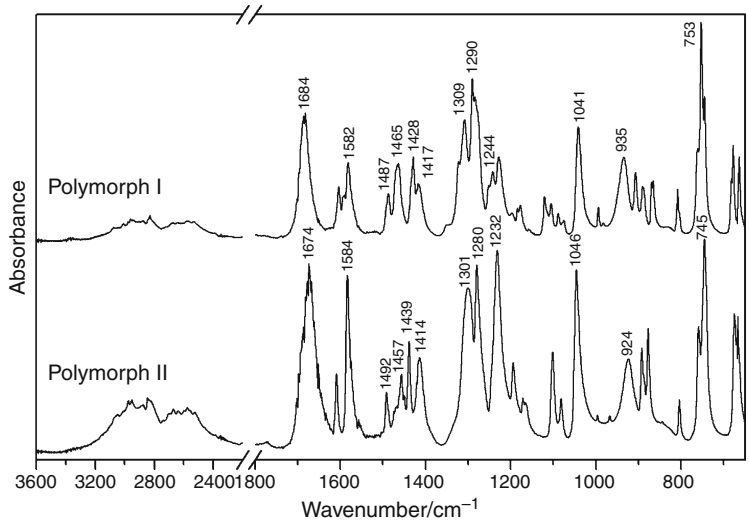


**Fig. 10** FTIR/ATR spectra of *m*-anisic acid polymorphic forms I and II

that the material obtained by crystallization in water solution at room temperature consists only of polymorph I.

After this confirmation of the polymorph composition of the powdered sample, we conducted XRPD heating/cooling experiments. A first diffractogram was collected at 20 °C for 1 h (Fig. 9). The capillary was then heated ($\beta \sim 6$ °C min$^{-1}$) until the melting of the sample at around 110 °C. After melting, the sample was cooled to

75 °C at a rate $\beta \sim 6$ °C min$^{-1}$, and XRPD data collection was conducted for 30 min at this temperature (Fig. 9). The sample was further cooled until 50 °C at the same rate, and data collection was performed at this temperature for 15 min. The diffractogram was very similar to the one obtained at 75 °C. Although the heating rates for XRPD and DSC are different, the diffractogram shown at 75 °C provides evidence of a new solid form, which we ascribe to polymorph II.

### *Fourier transform infrared spectroscopy*

As milling, even for KBr pellet preparation, induces polymorphic transition from form II to form I, a less aggressive technique was used, FTIR/ATR, to obtain the infrared spectra of both polymorphs (see Fig. 9).

As expected in the infrared spectra of polymorphic forms, some spectral differences in the intensity and position of the bands are observed, particularly in those bands associated with functional groups involved in hydrogen bonds.

The spectroscopic and theoretical studies of *m*-anisic acid polymorph I [41, 42] allow the assignment of some selected bands of polymorph II identified in Fig. 10 by their wavenumbers. These are presented in Table 5.

Several empirical equations relate the enthalpy, $\Delta H$, of hydrogen bonds to the shift of the bands relatively to the free molecule band frequency values [43–45]. In *m*-anisic acid, the blue shift of the hydroxyl group out of plane bending mode, $\gamma$(OH), is a good indicator of the strength of the hydrogen bonds. Applying the Rozenberg equation ($-\Delta H = 0.67 \times 10^{-4} \times [(\gamma(\mathrm{OH})_H)^2 - (\gamma(\mathrm{OH})_0)^2]$) [45], the value $-35$ kJ mol$^{-1}$ is obtained for polymorph I and $-33$ kJ mol$^{-1}$ for polymorph II. These are in agreement with the presence of strong hydrogen bonds in both polymorphs. In these calculations, $\gamma(\mathrm{OH})_0$ was taken as 596 cm$^{-1}$. This frequency was obtained from ab initio calculations performed on the isolated B molecule. The calculated vibrational frequencies were scaled by the recommended factor of 0.9613 [46].

According to the empirical rules developed by Burger and Ramberger [47, 48], it is possible to classify this system as a monotropic one. We note that polymorph II melts at $T_{fus} = 94.0$ °C with enthalpy value of $\Delta_{fus}H = 19.8$ kJ mol$^{-1}$, these values are smaller than those of polymorph I that melts at $T_{fus} = 105.4$ °C with enthalpy of $\Delta_{fus}H = 23.2$ kJ mol$^{-1}$. Infrared spectra show that the hydrogen bond network of polymorph I is stronger than that of polymorph II. Finally, the conversion of polymorph II into polymorph I after some elapsed time reveals that the most stable form at room temperature is polymorph I.

**Table 5** *m*-Anisic acid polymorphs I and II: assignment of infrared bands identified in Fig. 10

| | Form I | Form II |
|---|---|---|
| $\nu$(C=O) | 1684 | 1674 |
| $\nu$(C=C) | 1608 | 1609 |
| $\nu$(C=C) | 1582 | 1584 |
| $\nu$(C=C) | 1487 | 1492 |
| $\delta(CH_3)$ | 1465 | 1457 |
| $\nu$(C=C) | 1428 | 1439 |
| $\delta$(OH) | 1417 | 1414 |
| $\nu$(C–OH) | 1290 | 1280 |
| $\gamma$(C–H) | 1244 | 1232 |
| $\nu(O–CH_3)$ | 1041 | 1046 |
| $\gamma$(OH) | 935 | 924 |
| $\delta$(C=O) | 808 | 804 |

**Table 6** *m*-Anisic acid solid forms obtained in the crystallization experiments

| Solvent | Temperature | Polymorph |
|---|---|---|
| Water | RT | I |
| Ethyl acetate | −2 °C | I |
| | RT | I |
| *n*-Hexane | RT | I |
| Ethanol | −2 °C | I |
| | RT | II > I |
| Ethanol/*n*-hexane (50/50, v/v) | RT | II + I |
| | RT[a] | II |
| Vapour diffusion of *n*-hexane into ethanol solution | RT | II > I |
| Vapour diffusion of carbon tetrachloride into ethanol solution | RT | II |

*RT* room temperature

[a] A slower evaporation rate was achieved using an Erlenmeyer flask

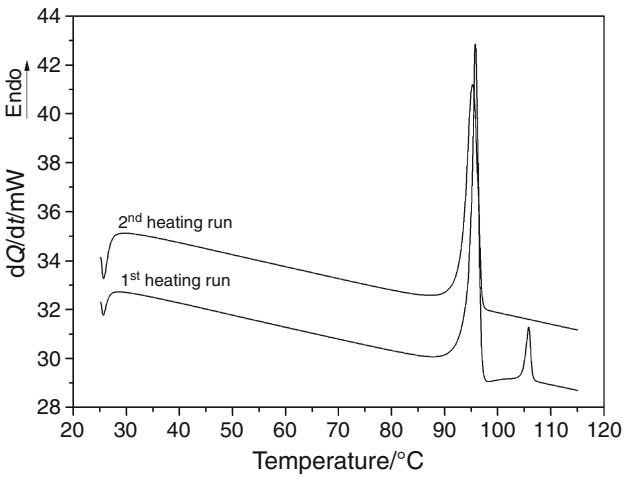


**Fig. 11** DSC curves of the first and second heating runs of *m*-anisic acid crystalized in ethanol solution at room temperature ($m = 1.22$ mg, $\beta = 10$ °C min$^{-1}$)

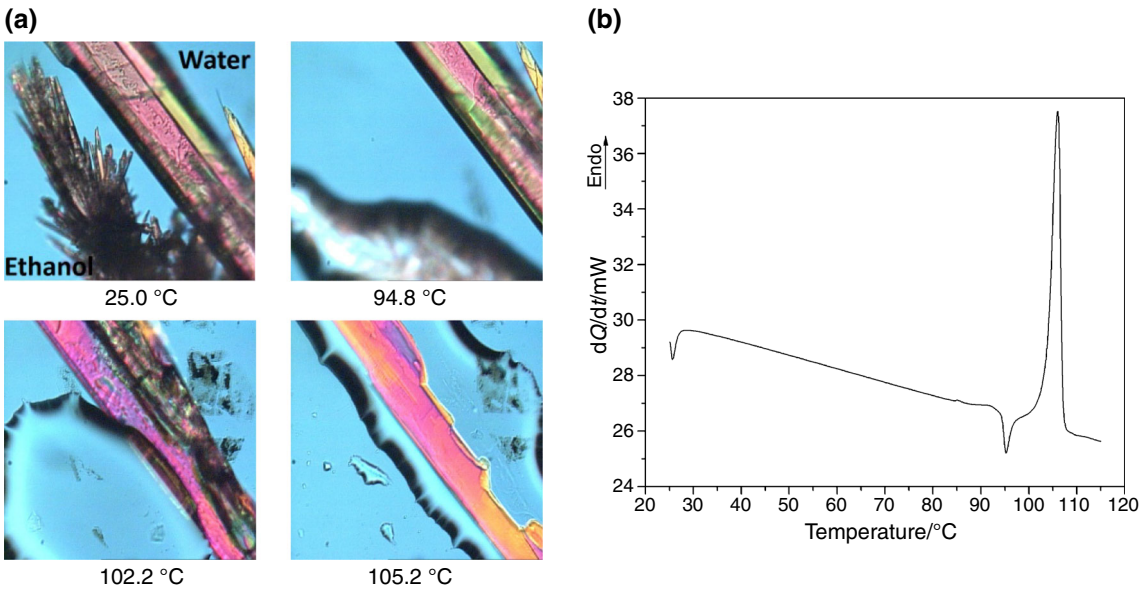


**Fig. 12** PLTM images (**a**) and DSC curve (**b**) of heating run of a *m*-anisic acid mixture of polymorph I and II obtained by crystallization in water and ethanol, respectively. ($\beta = 10$ °C min$^{-1}$, ×200 and $m = 1.20$ mg)

*Solid samples obtained by crystallization from solutions*

Crystallization from several solvents (water, ethanol, ethyl acetate, *n*-hexane) induced by solvent evaporation under different temperature conditions (room temperature and 2 °C) and also by vapour diffusion (*n*-hexane into ethanol solution) was carried out. The resulting solids were analysed by DSC and PLTM for the identification of the polymorphic form, and the results are presented in Table 6. Although the best crystals were analysed by SXD, all the single crystals of polymorph II were too thin for a data collection.

Considering the thermal analysis results, special attention should be made to the DSC curve obtained for the sample crystallized from ethanol at room temperature, Fig. 11. The presence of polymorph II concomitantly with a small amount of polymorph I leads to this DSC curve where melting of polymorph II is followed by a small crystallization event and afterwards by melting of polymorph I. A second heating cycle of these samples shows the normal melting of polymorph II.

Further information was obtained by PLTM, a good technique to follow polymorphic behaviour [49–52]. Polymorph I (crystals obtained in water at room temperature) and II (crystals obtained in ethanol at room temperature) were joined in the same microscopic field, and their thermal behaviour was observed, Fig. 12.

The images reveal melting of polymorph II at 95 °C and melting of polymorph I at 105 °C without observation of crystallization of the liquid. This experiment reveals that the crystallization process of the liquid in contact with solid form I is kinetically rather slow, even though it is thermodynamically favourable under these conditions. However, in DSC conditions for the same sample, melting of polymorph I is the major event observed.

## Conclusions

An investigation on the polymorphism of *m*-anisic acid, a GRAS flavouring substance, was undertaken. The presence of two conformers in polymorph I unit cell is a rare case of conformational isomorphism. A new solid form, polymorph II, was also identified and characterized. Thermal analysis data, infrared spectra and time evolution allow ascribing a monotropic relationship between polymorphs I and II. Polymorph I is the stable form under ambient conditions.

## Supplementary material

Crystallographic data for the structure reported in this paper have been deposited at the Cambridge Crystallographic Data Center number, CCDC 985352. Copies of this information may be obtained free of charge on application to CCDC, 12 Union Road, Cambridge CB2 1EZ, UK (fax: +44 1223 336 033; e-mail: deposit@ccdc.cam.ac.uk or http://www.ccdc.cam.ac.uk).

**Acknowledgements** P. S. Pereira Silva acknowledges the support by Fundação para a Ciência e a Tecnologia, under the scholarship SFRH/BPD/84173/2012. The Center for Pharmaceutical Studies (CEF), the Coimbra Chemistry Centre (CCC) and Centro de Estudos de Materiais por Difracção de Raios-X (CEMDRX) are supported by the Fundação para a Ciência e a Tecnologia (FCT), Portuguese Agency for Scientific Research, through the projects PEst-OE/SAU/UI0177/2014, PEst-OE/QUI/UI0313/2014 and PEst-C/FIS/UI0036/2011, respectively.

## References

1. Scientific opinion on flavouring group evaluation 96 (FGE.96). EFSA J. 2011;9(12):1924:1–60.
2. Food Agriculture Organization. Evaluation of certain food additives and contaminants—WHO Technical Report Series 909. Switzerland: World Health Organization; 2002.
3. Gunn ET, Bonner P, Santora D, inventors. Skin care composition, useful e.g. for providing moisture to mammalian skin, comprises oil, water, emulsifier and preservative comprising organic acid e.g. benzoic acid, *p*-anisic acid, sorbic acid, lactic acid, acetic acid or formic acid. USA patent US2011152384-A1. 2011.
4. Peters AF, inventor Pk Peters Krizman Sa, assignee. Composition useful as medicine for preventing and/or treating infection, preferably vaginal infection, bacterial infection and/or fungal infection, comprises anisic acid or its derivative and/or salt, and acid buffer. EU patent EP2314283-A1. 2011.
5. Capelli C, inventor Capelli Cristina, assignee. Antiseptic agent composition, use and preparation thereof, and formulation containing the same are disclosed. Japão patent JP2010270083-A. 2010.
6. Papageorgiou S, Varvaresou A, Tsirivas E, Demetzos C. New alternatives to cosmetics preservation. J Cosmet Sci. 2010;61(2):107–23.
7. Perlovich GL, Volkova TV, Manin AN, Bauer-Brandl A. Extent and mechanism of solvation and partitioning of isomers of substituted benzoic acids: a thermodynamic study in the solid state and in solution. J Pharm Sci. 2008;97(9):3883–96. doi:10.1002/jps.21260.
8. Callanan JE, Sullivan SA, Vecchia DF. Standards development for differential scanning calorimetry. J Res Natl Bur Stand. 1986;91(3):123–9.
9. Parvez M. Structure of *o*-anisic acid. Acta Crystallogr, Sect C. 1987;43(11):2243–5. doi:10.1107/S0108270187088231.
10. Fausto R, Matos-Beja A, Paixao JA. Molecular structure and charge density analysis of p-methoxybenzoic acid (anisic acid). J Mol Struct. 1997;435(3):207–18. doi:10.1016/s0022-2860(97)00187-7.
11. Raffo PA, Rossi L, Alborés P, Baggio RF. Cukiernik FD (2014) Alkoxy-benzoic acids: some lacking structures and rationalization of the molecular features governing their crystalline architectures. J Mol Struct. 2014;1070(0):86–93. doi:10.1016/j.molstruc.2014.04.003.
12. Lohani S, Grant DJW. Thermodynamics of polymorphs. In: Hilfiker R, editor. Polymorphism: in the pharmaceutical industry. Weiheim: Wiley VCH; 2006. p. 21–42.
13. McCrone WC. Polymorphism. In: Fox D, Labes MM, Weissberger A, editors. Physics and chemistry of the organic solid state. New York: Wiley Interscience; 1965. p. 725–67.
14. Bilton C, Howard JAK, Madhavi NNL, Nangia A, Desiraju GR, Allen FH, et al. When is a polymorph not a polymorph? Helical trimeric O–H center dot center dot center dot O synthons in trans-1,4-diethynylcyclohexane-1,4-diol. Chem Commun. 1999;17:1675–6. doi:10.1039/a905025f.
15. Esteves de Castro RA, Canotilho J, Barbosa RM, Silva MR, Beja AM, Paixa JA, et al. Conformational isomorphism of organic crystals: racemic and homochiral atenolol. Cryst Growth Des. 2007;7(3):496–500. doi:10.1021/cg0601857.
16. Maria TMR, Castro RAE, Bebiano SS, Silva MR, Beja AM, Canotilho J, et al. Polymorphism of trans-1,4-cyclohexanediol: conformational isomorphism. Cryst Growth Des. 2010;10(3):1194–200. doi:10.1021/cg901160v.
17. Newberne P, Smith RL, Doull J, Feron VJ, Goodman JI, Munro IC, et al. GRAS flavoring substances 19. Food Technology. 2000;54(6):66–84.
18. Sabbah R, An XW, Chickos JS, Leitao MLP, Roux MV, Torres LA. Reference materials for calorimetry and differential thermal analysis. Thermochim Acta. 1999;331(2):93–204. doi:10.1016/s0040-6031(99)00009-x.
19. Della Gatta G, Richardson MJ, Sarge SM, Stolen S. Standards, calibration, and guidelines in microcalorimetry—Part 2. Calibration standards for differential scanning calorimetry—(IUPAC Technical Report). Pure Appl Chem. 2006;78(7):1455–76. doi:10.1351/pac200678071455.
20. Bruker. APEX2 and SAINT. Madison: Bruker AXS Inc.; 2003.
21. Sheldrick GM. SADABS. Germany: University of Göttingen; 2003.
22. Sheldrick GM. A short history of SHELX. Acta Crystallogr, Sect A. 2008;64:112–22. doi:10.1107/s0108767307043930.
23. A. GA. PC GAMESS/Firefly version 7.1.G. 2009. http://classic.chem.msu.su/gran/gamess/index.html.
24. Schmidt MW, Baldridge KK, Boatz JA, Elbert ST, Gordon MS, Jensen JH, et al. General atomic and molecular electronic-structure system. J Comput Chem. 1993;14(11):1347–63. doi:10.1002/jcc.540141112.
25. Becke AD. Density functional exchange energy approximation with correct asymptotic behavior. Phys Rev A. 1988;38(6):3098–100. doi:10.1103/PhysRevA.38.3098.
26. Becke AD. Density functional thermochemistry. 3. The role of exact exchange. J Chem Phys. 1993;98(7):5648–52. doi:10.1063/1.464913.
27. Lee CT, Yang WT, Parr RG. Development of the Colle-Salvetti correlation-energy formula into a functional of the electron-density. Phys Rev B. 1988;37(2):785–9. doi:10.1103/PhysRevB.37.785.
28. Steiner T. Frequency of Z' values in organic and organometallic crystal structures. Acta Crystallogr, Sect B. 2000;56:673–6. doi:10.1107/s0108768100002652.
29. Desiraju GR. On the presence of multiple molecules in the crystal asymmetric unit (Z[prime or minute] > 1). Chem Eng Commun. 2007;9(1):91–2. doi:10.1039/B614933B.
30. Anderson KM, Steed JW. Comment on "On the presence of multiple molecules in the crystal asymmetric unit (Z[prime or minute] > 1)" by Gautam R. Desiraju, CrystEngComm, 2007, 9, 91. Chem Eng Commun. 2007;9(4):328–30. doi:10.1039/B701009E.
31. Etter MC. Encoding and decoding hydrogen bond patterns of organic compounds. Acc Chem Res. 1990;23(4):120–6. doi:10.1021/ar00172a005.
32. Bernstein J, Davis RE, Shimoni L, Chang NL. Patterns in hydrogen bonding—functionality and graph set analysis in crystals. Angew Chem Int Ed. 1995;34(15):1555–73. doi:10.1002/anie.199515551.
33. McKinnon JJ, Mitchell AS, Spackman MA. Hirshfeld surfaces: a new tool for visualising and exploring molecular crystals. Chem Eur J. 1998;4(11):2136–41. doi:10.1002/(sici)1521-3765(19981102)4:11<2136:aid-chem2136>3.0.co;2-g.
34. McKinnon JJ, Spackman MA, Mitchell AS. Novel tools for visualizing and exploring intermolecular interactions in molecular crystals. Acta Crystallogr, Sect B. 2004;60:627–68. doi:10.1107/s0108768104020300.

35. Wolff SK, Griwood DJ, McKinnon JJ, Turner MJ, Jayatilaka D, Spackman MA. CrystalExplorer (version 3.1). Perth: University of Western Australia; 2012.
36. Buttar D, Charlton MH, Docherty R, Starbuck J. Theoretical investigations of conformational aspects of polymorphism. Part 1: *O*-acetamidobenzamide. J Chem Soc Perkin Trans. 2. 1998; 763–72. doi:10.1039/a706978b.
37. Desiraju GR, Steiner T. The weak hydrogen bond. Oxford: Oxford University Press; 1999.
38. Mullin JW. Crystallization. 4th ed. Oxford: Butterworth-Heinemann; 2001.
39. Young RA. The Rietveld method. Oxford: Oxford University Press; 1993.
40. Rodriguezcarvajal J. Recent advances in magnetic-structure determination by neutron powder diffraction. Phys B. 1993;192(1–2): 55–69. doi:10.1016/0921-4526(93)90108-i.
41. Kalinowska M, Swislocka R, Rzaczynska Z, Sienkiewicz J, Lewandowski W. Spectroscopic (FT-IR, FT-Raman, UV, (1)H, and (13)C NMR) and theoretical studies of *m*-anisic acid and lithium, sodium, potassium, rubidium, and caesium *m*-anisates. J Phys Org Chem. 2010;23(1):37–47. doi:10.1002/poc.1581.
42. Varsányi G. Assignments for vibrational spectra of 700 benzene derivatives. Budapest: Akadémiai Kiadó; 1973.
43. Iogansen AV. Direct proportionality of the hydrogen bonding energy and the intensification of the stretching v(XH) vibration in infrared spectra. Spectrochim Acta, Part A. 1999;55(7–8):1585–612. doi:10.1016/s1386-1425(98)00348-5.
44. Stolov AA, Borisover MD, Solomonov BN. Hydrogen bonding in pure base media. Correlations between calorimetric and infrared spectroscopic data. J Phys Org Chem. 1996;9(5):241–51. doi:10.1002/(sici)1099-1395(199605)9:5<241:aid-poc782>3.0.co;2-c.
45. Rozenberg MS. IR spectra and hydrogen bond energies of crystalline acid salts of carboxylic acids. Spectrochim Acta, Part A. 1996;52(11):1559–63. doi:10.1016/0584-8539(96)01703-5.
46. Foresman JB, Frisch A. Exploring chemistry with electronic structure methods. 2nd ed. Pittsburgh: Gaussian, Inc.; 1996.
47. Burger A, Ramberger R. On the polymorphism of pharmaceuticals and other molecular crystals. I. Mikrochim Acta. 1979;II:259–71.
48. Burger A, Ramberger R. On the polymorphism of pharmaceuticals and other molecular crystals. II. Mikrochim Acta. 1979;II:273–316.
49. Maria TR, Castro RE, Silva MR, Ramos ML, Justino LG, Burrows H, et al. Polymorphism and melt crystallisation of racemic betaxolol, a β-adrenergic antagonist drug. J Therm Anal Calorim. 2013;111(3):2171–8. doi:10.1007/s10973-012-2765-9.
50. Arranja C, Marcos M, Silva M, Eusébio ME, Castro RE, Sobral AFN. Synthesis and polymorphism evaluation of the 3,5-bis(decyloxy)benzaldehyde. J Therm Anal Calorim. 2014;117(3):1375–83. doi:10.1007/s10973-014-3904-2.
51. Gálico DA, Perpétuo GL, Castro RAE, Treu-Filho O, Legendre AO, Galhiane MS, et al. Thermoanalytical study of nimesulide and their recrystallization products obtained from solutions of several alcohols. J Therm Anal Calorim. 2014;115(3):2385–90. doi:10.1007/s10973-013-3294-x.
52. Abu Bakar M, Nagy Z, Rielly C. A combined approach of differential scanning calorimetry and hot-stage microscopy with image analysis in the investigation of sulfathiazole polymorphism. J Therm Anal Calorim. 2010;99(2):609–19. doi:10.1007/s10973-009-0001-z.